Journal of Renewable Materials

Tech Science Press

DOI: 10.32604/jrm.2020.012782

ARTICLE

Performance of Unidirectional Biocomposite Developed with *Piptadeniastrum Africanum* Tannin Resin and *Urena Lobata* Fibers as Reinforcement

Achille Gnassiri Wedaïna[1,2], Antonio Pizzi[2], Wolfgang Nzie[1], Raidandi Danwe[3], Noel Konaï[4,*], Siham Amirou[2], Cesar Segovia[5] and Raphaël Kueny[5]

[1]Laboratory of Mechanics, Materials, and Modelization (PAI), University of Ngaoundéré, Ngaoundéré, 454, Cameroon

[2]Laboratory of Studies and Research on Wood Material (LERMAB), University of Lorraine, Epinal, 88000, France

[3]Laboratory of Mechanics, Materials and Building, University of Maroua, Maroua, Cameroon

[4]Laboratory of Materials Mechanics, University of Yaoundé 1, Yaoundé, 8390, Cameroon

[5]Lorrain Textile Test Center (CETELOR), University of Lorraine, Epinal, 88026, France

*Corresponding Author: Noel Konaï. Email: noel.konai@yahoo.fr

Received: 12 July 2020 Accepted: 21 September 2020

ABSTRACT

The *Piptadeniastrum Africanum* bark tannin extract was characterized using MALDI TOF, ATR-FT MIR. It was used in the development of a resin with *Vachellia nilotica* extract as a biohardener. This tannin is consisting of Catechin, Quercetin, Chalcone, Gallocatechin, Epigallocatechin gallate, Epicatechin gallate. The gel time of the resin at natural pH (pH = 5.4) is 660 s and its MOE obtained by thermomechanical analysis is 3909 MPa. The tenacity of *Urena lobata* fibers were tested, woven into unidirectional mats (UD), and used as reinforcement in the development of biocomposite. The fibers tenacity at 20, 30 and 50 mm lengths are respectively 65.41, 41.04 and 33.86 $cN{\cdot}Tex^{-1}$. The UD biocomposite obtained had very interesting mechanical properties. Its density, tensile MOE, ultimate strength, bending MOE and MOR are respectively 926 $kg{\cdot}m^{-3}$, 6 GPa, 55 MPa, 9.3 GPa and 68.3 MPa. This biocomposite can be used in a building exterior structure.

KEYWORDS

Adhesive; biocomposite; fibers; hardener; MOE and MOR

1 Introduction

Nowadays, the development of degradable composite reinforced with biofibers is of crucial importance. Biofibers such as natural fibers offer several advantages: low density, low cost, environment protection and high specific mechanical performance, which makes it a substitute for synthetic glass, carbon and other synthetic fibers. Biocomposites were developed in all sectors of society, particularly in the aeronautics, automotive and wood industries etc. Recently, high-performance composite materials using biofibers have been developed [1–6]. The reinforcements have an essential function because they ameliorated the mechanical characteristics of composites: rigidity, tensile resistance, bending resistance and hardness [7–9]. These reinforcements also allow to upgrade thermal behavior, temperature resistance, fire resistance, abrasion resistance, electrical properties, environmental properties, optical properties, and acoustical properties. Fibers are commercialized in various forms: Linear (yarn, roving, tow), woven

(braids, complex fabrics), non-woven and particles [7]. Synthetic resins, developed from oil waste that generates toxic gases with a direct impact on the destruction of the ozone layer [10,11] are being replaced by bioadhesive [6,12]. Substances such as formaldehyde, which is a hardener commonly used in synthetic resins, carcinogenic and harmful [13]. make the materials entirely bio, several research works have developed adhesives of animal and vegetable based origin [14,15]. Resins based on tannins, lignins or proteins have been developed as adhesives for wood, and have been used to develop composite materials with good environmental properties [12,16,17]. It should be noted that synthetic hardeners such as formaldehyde, glyoxal, hexamine, are used but in small proportions. In previous work, the company STRAMIT has succeeded the production of straw panels by thermocompression without the use of any adhesive [18]. Renewable agricultural products, composite sheets and 100% vegetable-based felts made from flax bonded with resins have also been developed [19] with good characteristics which can be improved by the use of binders. Tannin-based resins have good compatibility with natural fibers. Recent work has developed biocomposites with tannin-resorcinol-formaldehyde and flax fiber [20]; with bast fibers such as flax, hemp, kenaf and jute [5] all with good mechanical properties.

In the interest of making composites fully bio-based, research has been carried out to substitute synthetic hardeners with biohardeners in tannin resins. A totally biohardeners derived from exudate extract of African trees *Vachellia nilotica* and *Senegalia senegal* has been studied [21] and then used to harden a maritime pine tannin resin without any aldehyde to obtain a biobased adhesive for interior particleboard [22]. The mechanical properties of totally bio-based composite using unidirectional woven mat is interesting to explore.

A totally bio and high-performance material could be less toxic to humans and environmental protection. The objective of this paper is to study the performance of a totally biocomposite based on a unidirectional woven mat and bio tannin adhesive.

2 Materials and Methods

2.1 Extraction of Urena Lobata Fibers

The *urena lobata* fibers used from a locality called Foulouwaina in the far north region of Cameroun more precisely in the Mayo Danay subdivision Yagoua. This town has a tropical Sudano-Sahelian climate and temperatures are high but with a great irregularity of rains; the dry season is longer than the rainy season [23]. the most precipitation lasts 4.4 months, from May 23 to October 3 and the driest season 7.6 months, from October 3 to May 23. So, the best time to harvest *Urena lobata* is from mid-September to December.

The *urena lobata* were extracted by fermentation and biological retting. The stems were cut, humidified and wrapped in a bag during three (3) weeks, then washed with water and dried at ambient temperature (25° C) during seven (7) days [24,25].

2.2 Extraction of Vachellia nilotica Exudats

The exudates of *Vachellia nilotica* were extracted in the forest of the Foulouwaina town. The bark trees were cut at several places at a depth of 0.5–1 centimeter and 30 s later from the wound came an organic solution of high viscosity. The exudates were then collected and dried at ambient temperature 21 days. Finally, the dried exudates were crushed to obtain a soluble whitish powder easier to stock and to use [26].

2.3 Tannin Extraction

The bark of *Piptadeniastrum Africanum* was collected by a forestry company in the city of Douala called "Interbois" located in Bonamoussadi district. The harvested and air-dried bark, grounded with a crushing machine into particles of 1.0 to 0.5 mm, was introduced into an aqueous solution containing 2% sodium bisulphite and 0.5% sodium bicarbonate (the ratio of water to bark was 6:1). Mixed at 60°C for 4 hours.

The solution was filtered using a special cloth to get a reddish black liquid and a solid residue. The recovered liquid fraction was then concentrated at 60°C using a rotary evaporator, then it was frozen using liquid nitrogen and spray dried using a laboratory spray dryer (Bowe Engineering) at 160°C and a flow rate of 10 ml·min^{-1}. A tannin powder, easier to use for analysis and storage was finally obtained [12].

2.4 Resin Formulation

In an aqueous solution containing 40% tannin of *Piptadeniastrum Africanumn*, introduce 15% *Vachellia nilotica*. Then mix for 10 minutes at 20°C until obtained homogeneous solution. [22]. All component weight was calculated on solids tannin, and pH of the mixture was not adjusted (pH = 5.4).

2.5 Preparation of Biocomposite

The fiber mats of 400 × 350 mm^2 size was made using a special device consisting of a rectangular frame made of solid wood, on which spikes are arranged at intervals of 5 mm. The weaving device used for process is showed in Figs. 6a and 6b. A fine cotton thread supplied by CETELOR was used to hold the fibers in the weft direction. Pre-combed fiber batches are aligned parallel and stretched across in the warp direction.

The pre-weighed carpets were impregnated with the resin by Scarf Impregnation (manufactured by Mathis, Zurich, Switzerland). The Passage was carried out six (6) times under a roller pressure of 4 MPa. The impregnation is considered correct when the resin reaches the fibers in the heart of the carpet. The pre-impregnated fabrics were weighed and placed under the hood at a temperature of 25°C for 5 hours and then weighed again.

The pressing of the biocomposite was done at 180°C, on a GOTTFRIED JOSS hydraulic press in tree steps during 8 min (4 min at 2 MPa pressure, 2 min at 1 MPa pressure and 2 min at 0.5 MPa pressure)

The biocomposite obtained contained 51% fiber and 49% resin.

2.6 Tannin Characterization

2.6.1 ATR-FT MIR Analysis

About 2 mg grinded powders of fine tannin extract was placed on the diamond/ZnSe crystal of the analytical device and contact is achieved by applying a hand force of approximately 150 N (manual force) on the sample. Each extract was scanned registering the spectrum with 32 scans with a resolution of 4 cm^{-1} in the range between 600 and 4000 cm^{-1}. The sample is scanned five times and the average of these spectra is studied in the fingerprint (4000 and 600 cm^{-1}) [12].

2.6.2 MALDI-TOF Analysis

Tannin for Laser Desorption Ionization Time-of-Flight (MALDI-TOF) mass spectrometry analysis was prepared by first dissolving 5 mg of tannin powder in 1 mL of a 50:50 v/v acetone/water solution. 10 mg of this solution was added to 10 µL of a 2-5-dihydroxy benzoic acid (DHB) matrix. To improve ion formation, NaCl was added to the matrix. The two previous solutions are mixed in a proportion of 50:50 and about 0.5 to 1 µl of this mixture is taken and placed on a wafer (around a spot). after evaporation of the solvent for a few minutes in the open air, the wafer is introduced into the spectrometer for further processing. The spectra were recorded in a KRATOS compact MALDI AXIMA PERFORMANCE TOF 2 instruments. The software MALDI-MS was used for data treatment [12,27–29].

2.7 Resin Characterization

2.7.1 Gel Time

5 g of liquid resin was introduced in a tube and placed in a water bath, maintained at boiling temperature (100°C) at normal atmospheric pressure. Spring has been inserted into the test tube and moved rapidly up and

down. The gelation time is measured by a stopwatch. The test is performed in three times and the mean value is reported [20,27].

2.7.2 Viscosity

To determine the viscosity, used a DV-II+ viscometer from Brookfield Engineering with a n° 5 spindle. The rotation speeds were 10, 20, 50, 100 rpm and the ambient temperature was 20°C [20,30].

2.7.3 Thermomechanical Analysis

The tests were carried out on a METTLER TOLEDO TMA/SDTA840 machine. About 25–30 mg of resin is placed on two Plywood with dimensions 17 × 5 × 1 mm and then glued. Place in the oven of the TMA Analyzer for testing. Samples are tested in non-isothermal flexure between 30°C and 250°C at a heating rate of 10°C/min. The resin was analyzed by three-point bending using an earlier technique [31,32]. The test was duplicated five times and the mean value was reported. The MOE values are obtained by measuring the change in deflection amplitude of the tested sandwich between the initial and final equilibrium deflection. The classical mechanical method of force-deflection relationship used Eq. (1):

$$E = \frac{L^3 \times F}{4bh^3(f_{wood} - f_{adhesive})} \tag{1}$$

where: E is Young's modulus, L = the length of the span tested, b is the width and h the thickness of the specimen, F is the force exerted on the tested assembly, f_{wood} and $f_{adhesive}$ are the deflections that have been proven to be constant and reproducible [21,33–35].

2.8 Fiber Bundle's Tenacity

The tenacity of bundle (mass m = 0.03 g, length 20, 30, and 50 mm) tested using the Instron 4206 machine according to NF G07-307 [36,37] with a feed rate of 1 mm/min. The linear mass in Tex, the tenacity of the beam in $cN{\cdot}Tex^{-1}$ and the relative elongation at break in % are deduced using formulae Eqs. (2)–(4) below respectively:

$$M = \frac{m}{L} \times 10^3 \tag{2}$$

$$R = \frac{F}{M} \tag{3}$$

$$E = \frac{A}{l} \times 100 \tag{4}$$

where L is fiber bundle length under pre-voltage (mm), l: length of the specimen measured between the jaws under pre-tension (mm), m: the mass of the specimen of length l (mg), M mass of the bundle (Tex), F is the breaking strength of the sample (cN), R is the tenacity ($cN{\cdot}Tex^{-1}$), A is breaking elongation (mm) and E is relative elongation at break (%).

2.9 Biocomposite Mechanical Characterization

2.9.1 Tensile Tests

Ten (10) specimens (ep_1 to ep_{10}) of 150 × 20 mm were tested according to NF ISO 527-4/2/1 [38] using an Instron 4206 universal testing machine. Values of the stress and strain were calculated respectively the following expressions Eqs. (5) and (6):

$$\sigma = \frac{F}{A} \tag{5}$$

$$\epsilon = \frac{\Delta L_0}{L_0} \tag{6}$$

where: F: strength causing a displacement (N), A: Area of the initial cross-section of the test piece (mm^2), L_0: length of the specimen (mm), ΔL_0: length of the test piece between the reference marks (mm).

The plots were drawn and using MATLAB software which allowed us to deduce the Young's Modulus (MOE), ultimate (R_m), yield (σ_y) and yield strain (ε_y).

2.9.2 Bending Tests

Ten (10) specimens of 80 × 25 mm were tested according to NF EN ISO 178 [39], using the Instron 4206 universal testing device at a speed of 2 mm/min and 20°C. The specimens have been numbered ep_1 to ep_{10}. The stresses and deformations were calculated the following expressions Eqs. (7) and (8) bellow:

$$\sigma = \frac{3PL}{2bh^2} \tag{7}$$

$$\epsilon = \frac{6hf}{L^2} \tag{8}$$

where: σ: normal stress (MPa): relative strain, f : deflection measured during the test for each load (mm), P: strength causing a displacement (N), L: between supports (mm), b: width of the sample (mm), h: of the sample (mm).

3 Results and Discussion

3.1 Tannin Characterization

The analysis of MALDI-TOF spectra of extract *Piptadeniastrum Africanum* tannin in Fig. 1 and Tab. 1 below, shows the existence of six monomers and oligomers in 20–2000 Da range. It is composed of Catechin (290.3 Da), Quercetin (302.2 Da), Chalcone (208.2 Da) Gallocatechin (306.2 Da), Epigallocatechin gallate (458.3 Da), Epicatechin gallate (442 Da) (Fig. 2). The peaks must be subtracted 23 Da to obtain the value of the molecular weight. This is due to the Na^+ enhancer used as NaCl in the matrix and bound to the oligomers to obtain the molar weight of the chemical species of the peak [12]. The loss of hydrogen atoms [40], the protonated forms [12] and the loss of hydroxyl groups [6] of the monomeric units to form the oligomers must be taken into account if they are not the terminal units of the oligomers. Condensation between molecules must be taken into account, as the water molecule will be removed from the oligomer during condensation [12]. Protonated or multi-protonated oligomers (with or without Na+) are present at 192, 232, 294, 316, 440, 441, 504, 507, 508, 746, 813, 946, 962, 977, 1078, 1109, 1534, 1568, 1694 Da. The protonated form is due to the presence of residual moisture in the analyzed sample and once the components are protonated, even if they are dry, they are still protonated [12]. Those who have lost or benefited from an OH group [27,41] are present at 550, 678, 854 Da.

The results indicate that Chalcone is the major constituent of the tannin of *Piptadeniastrum Africanum*

The analysis of the ATR FT-MIR spectrum in the region between 4000 and 600 cm^{-1} (Fig. 3) reveals the presence of several functional groups which are typical for condensed and hydrolysable tannins (Tab. 2). Aromatic torsions, but especially out-of-plane C-H bends, are assigned to the 618 cm^{-1} band. The band at 1606 cm^{-1} is associated aromatic vibrations mainly C = C in the aromatic rings [42]. Model compounds suggest that, this type of signal is more common in species containing aromatic rings with two hydroxyl groups. This hypothesis suggests that the extract may contain a majority of (meta)di-hydroxy aromatics [43] Bands near 3134 cm^{-1} are to the O–H of carboxylic acids.

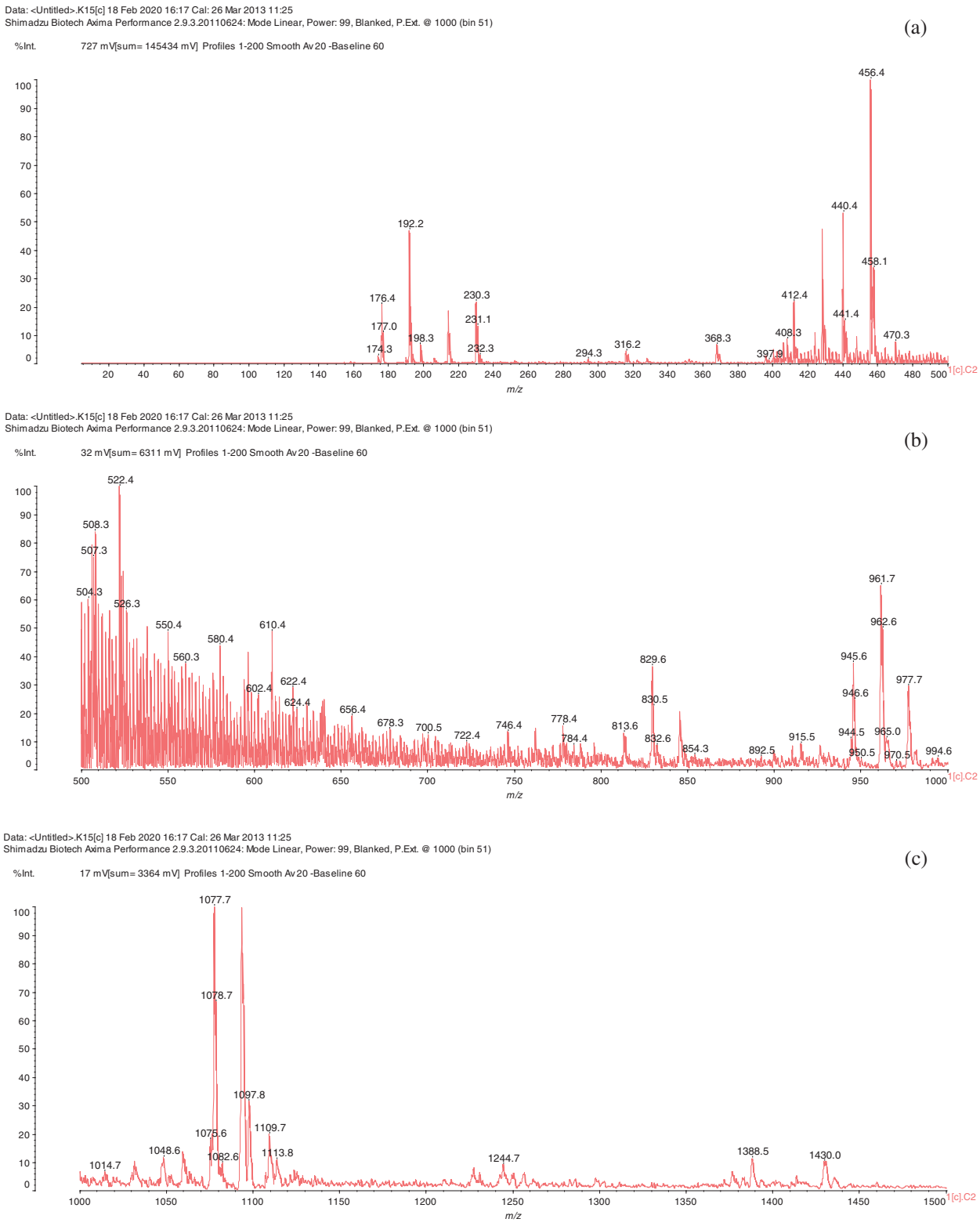

Figure 1: (continued)

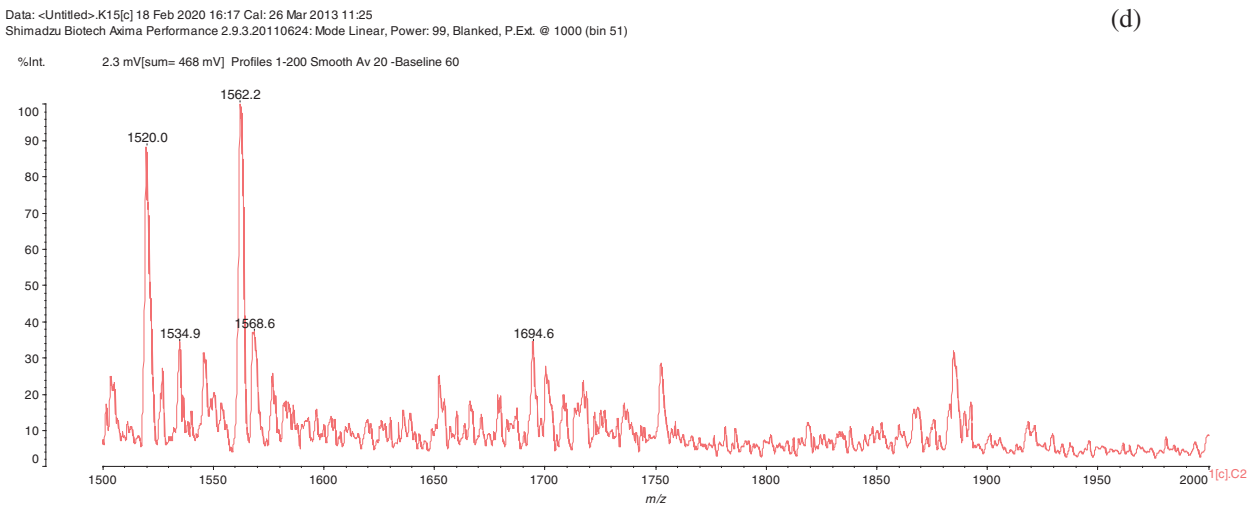

Figure 1: MALDI ToF of the *Piptadeniastrum africanum* tannin: (a) 20 Da–500 Da range. (b) 500 Da–1000 Da range. (c) 1000 Da–1500 Da range. (d) 1500 Da–2000 Da range

Table 1: Monomers and oligomers present in the tannin of *Piptadeniastrum Africanum*

Pics (g/mol)	Monomer	Remark
192	gallic acid + Na (+2H)	Monomer
198	Glucose + H_2O	Monomer
230	Chalcone + Na (-H)	Flavonoid monomer
294	Catéchin tétraprotoneted	Flavonoid monomer
316	Catéchin tétraprotoneted + Na	Flavonoid monomer
368	Chalcone + glucose (-H_2O)	Flavonoid-glucose dimer
397	Chalcone + gallic acid + Na	Flavonoid + fragment
408	Chalcone + glucose + Na	Flavonoid-glucose dimer
412	Chalcone dimer (-2H)	Flavonoid dimer
440	Chalcone dimer triprotoneted + Na	Flavonoid dimer
456	Gallocatéchin gallatte (-2H)	Flavonoid monomer
470	Quercétine gallate	Flavonoid monomer
504	Quercétin diprotoneted + glucose + Na	Flavonoid-glucose dimer
508	Epigallocatéchin diprotoneted + glucose + Na	Flavonoid-glucose dimer
522	Catéchine tétraprotoneted + Chalcone + Na	Flavonoid dimer
526	Quercétine + Chalcone + Na (-3H)	Flavonoid dimer

(Continued)

Table 1 (continued).

Pics (g/mol)	Monomer	Remark
550	Epigallocatéchine + Chalcone + Na (+OH)	Flavonoid dimer
560	Catéchine dimer (-H2O)	Flavonoid dimer
580	Catéchine dimer	Flavonoid dimer
602	Catechin dimer + Na	Flavonoid dimer
610	Epigallocatechin dimer	Flavonoid dimer
622	Quercetin dimer + Na (-2H)	Flavonoid dimer
624	Quercetin dimer protoneted + Na	Flavonoid dimer
656	Gallocatechin galate + glucose + Na (-H)	Flavonoid dimer
678	Gallocatechin galate + Chalcone (+OH)	Flavonoid dimer
700	Chalcone dimer + catéchine (-2H)	Flavonoid trimer
722	Chalcone dimer + catéchine + Na (-H)	Flavonoid trimer
746	Epicatechin gallate diprotonated + Quercetin	Flavonoid dimer
778	catechin dimer + glucose + Na	Flavonoid trimer
784	catéchin dimer + Chalcone	Flavonoid trimer
813	Chalcone Protonated+ Quercétine + Epigallocatechin + Na	Flavonoid trimer
829	Chalcone tetramer (-3H)	Flavonoid tetramer
832	Chalcone tetramer	Flavonoid tetramer
854	Catechin trimer (-OH)	Flavonoid trimer
892	Gallocatechin galate protonated + Chalcone dimer + Na+	Flavonoid trimer
915	Epigallocatechin trimer protonated	Flavonoid trimer
945	Chalcone trimer + Epigallocatechine + Na	Flavonoid tetramer
961	Epigallocatechin+ Gallocatechin galate + glucose + Na	Flavonoid dimer +glucose
965	Epicatechin gallate + Quercetin + Chalcone + Na (-3H)	Flavonoid trimer
970	Epicatechin gallate + Epigallocatechin + Chalcone + Na (-3H)	Flavonoid trimer
977	Epicatechin gallate tetraprotonated + Epigallocatechin + Chalcone + Na	Flavonoid trimer
994	Quercetin + Chalcone + catechin + Na (-H)	Flavonoid trimer
1014	Chalcone tetramer + gallic acid + Na (-H)	Flavonoid tetramer +fragment
1048	Epicatechin gallate + Quercetin + Catéchine + Na (-3H)	Flavonoid trimer
1075	Gallocatechin gallate + Quercétin dimer + Na (-4H)	Flavonoid trimer
1077	Gallocatechin gallate + Quercetine dimer + Na (-2H)	Flavonoid trimer
1082	Gallocatéchin gallate + Epigallocatéchin + Quercétine + Na	Flavonoid trimer
1097	Gallocatechin gallate + Epicatechin gallate + glucose + Na	Flavonoid dimer +glucose

(Continued)

Table 1 (continued).

Pics (g/mol)	Monomer	Remark
1109	Catechin dimer + Quercetin + Chalcone diprotonated + Na	Flavonoid tetramer
1109	Catechin dimer + Quercetin + Chalcone diprotonated + Na	Flavonoid tetramer
1113	Quercetin dimer + Chalcone + catechin + Na (-2H)	Flavonoid tetramer
1244	Catechin dimer + Chalcone + Epicatechin gallate + Na (-H)	Flavonoid tetramer
1388	Gallocatechin gallate trimer + Na(-3H)	Flavonoid trimer
1430	Quercetin tetramer + Chalcone + Na (-H)	Flavonoid tetramer
1520	Quercetin dimer + Epigallocatechin dimer + catechin + Na (-H)	Flavonoid pentamer
1534	Quercetin trimer protonated + Epigallocatechin dimer + Na	Flavonoid pentamer
1562	Epigallocatechin pentamer + Na (+OH)	Flavonoid pentamer
1568	Epicatechin gallate dimer triprotonated + Gallocatechin galate + Chalcone + Na	Flavonoid tetramer
1694	Gallocatechin gallate trimer + Epigallocatechin protonated + Na	Flavonoid tetramer

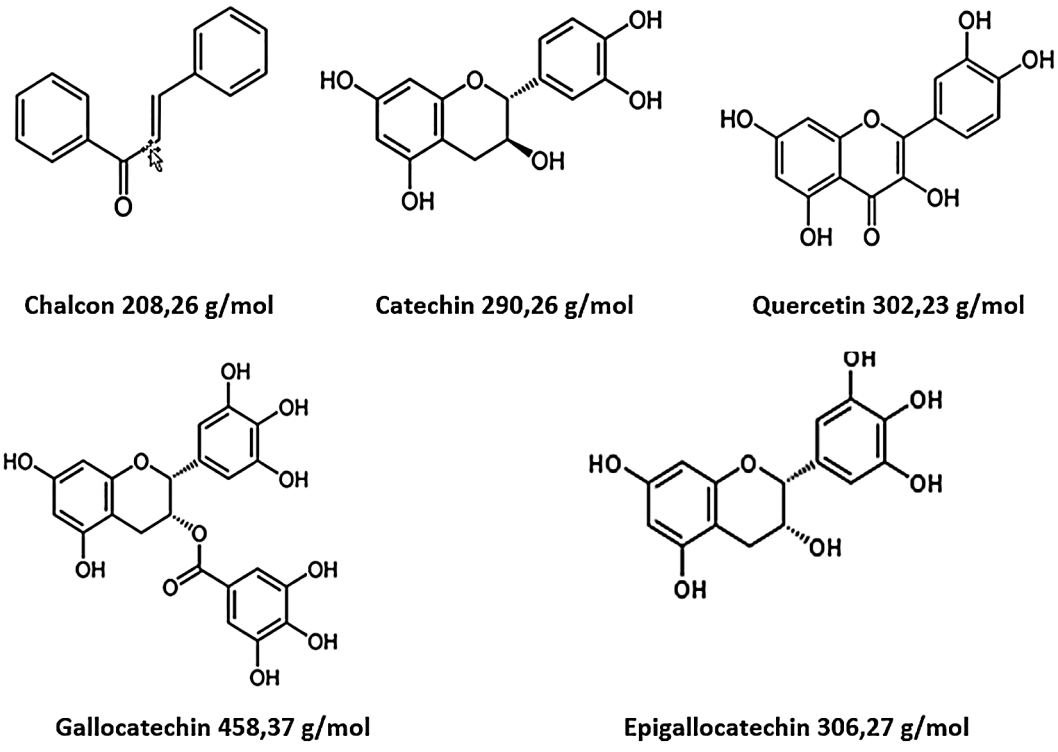

Figure 2: Monomers structures present in *Piptadeniastrum Africanum* tannin extract

3.2 Gel Time and Thermomechanical Analysis (TMA)

The gel time was measured at the natural pH (pH = 5.4). It gels in 660 s, faster than pine resin (1490 s) (with the same *vachellia nilotica* hardener) [21]. It means that the tannin of *Piptadeniastrum Africanum* is more reactive with this hardener.

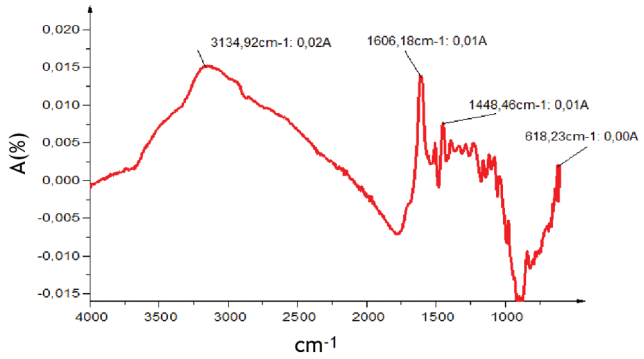

Figure 3: ATR-FT MIR spectrum of *Piptadeniastrum Africanum* tannin extract

Table 2: Results summary of ATR-FT MIR

Pic (ppm)	Assignment
618	Aromatic torsion, out-of-plane C-H bending
1448	C-H Aromatic bending, tetrahedral carbon, C-O stretching, and C-OH deformation
1606	Vibratory movements of the C = C groups in the aromatic rings
3134	O-H carboxylic acids

The curve in Fig. 4 shows the variation of MOE as a function of the temperature of the resin formulated with *Piptadeniastrum Africanum* tannin and *Vachellia nilotica* hardener. The observation of this curve shows three phases: Evaporation, hardening and degradation. The curing process of the resin started at 100°C to 150°C, during this range considerate as polycondensation reaction, the molecular range increased.

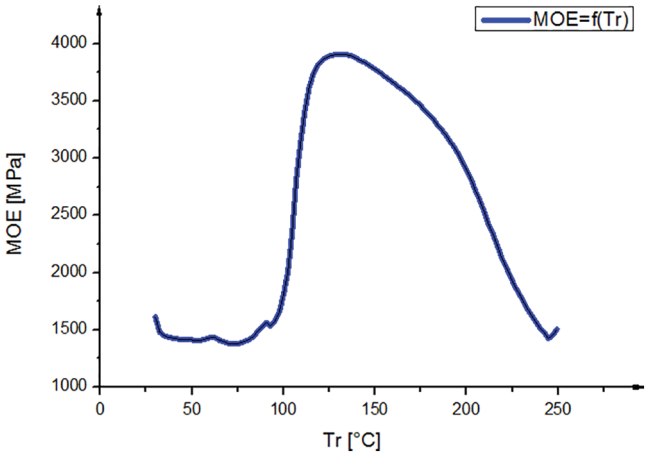

Figure 4: TMA curve of the bio resin

3.3 Elaboration and Mechanical Characterization of the Composite

3.3.1 Fiber Tenacity

The standard deviations of different fibers lengths serials (L = 20 mm, 30 mm, 50 mm) are calculated, their values are mentioned in Tab. 3 and plotted on histogram (red color values) Figs. 5a and 5b. The

tenacities values of these different lengths are respectively 65.41; 41.04; 33.86 cN·Tex^{-1} and their standards deviations are respectively 1.3; 0.91 and 0.7. As the fiber is longer, its tenacity is reduced. This could be explained by the fiber has a minimum length of 2 cm, the longer the fiber is long its linear mass becomes important [44]. The rupture elongation of the fibers decreases as the length increases. the different tenacity values are slightly high compared to those of jute (26.5–51.2 [45]), Sisal (35.3–44.1 [45–47]), Cotton (24–43.3 [45,46,48]) and Alfa (6.5–19.3 [7]). The fibers extraction method could have an impact on tenacity.

Table 3: Tenacity of different length fiber

Length	L = 20 mm	L = 30 mm	L = 50 mm
Tenacity (cN/Tex)	65.41	41.04	33.86
Std	1.3	0.91	0.7

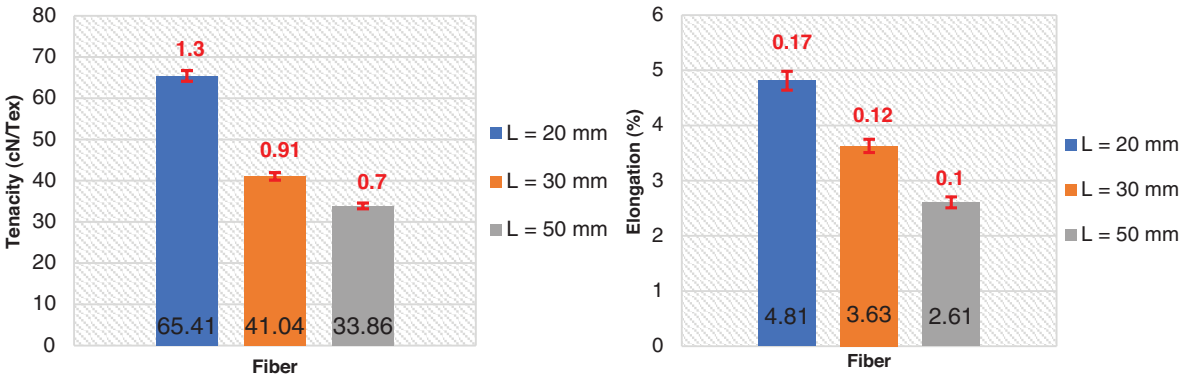

(a) (b)

Figure 5: (a) Tenacity of *urena Lobata* fiber bundles; (b) Elongation at break of *urena Lobata* fiber bundles

(a) (b)

Figure 6: (a) Weaving equipment (b) Fiber arrangement

3.3.2 Biocomposite Elaboration

After weaving we obtain unidirectional mat of *urena lobata* fiber (Fig. 7). the woven mat dimensions and weight are respectively 400 × 350 mm^2 and 182 $g{\cdot}m^{-2}$.

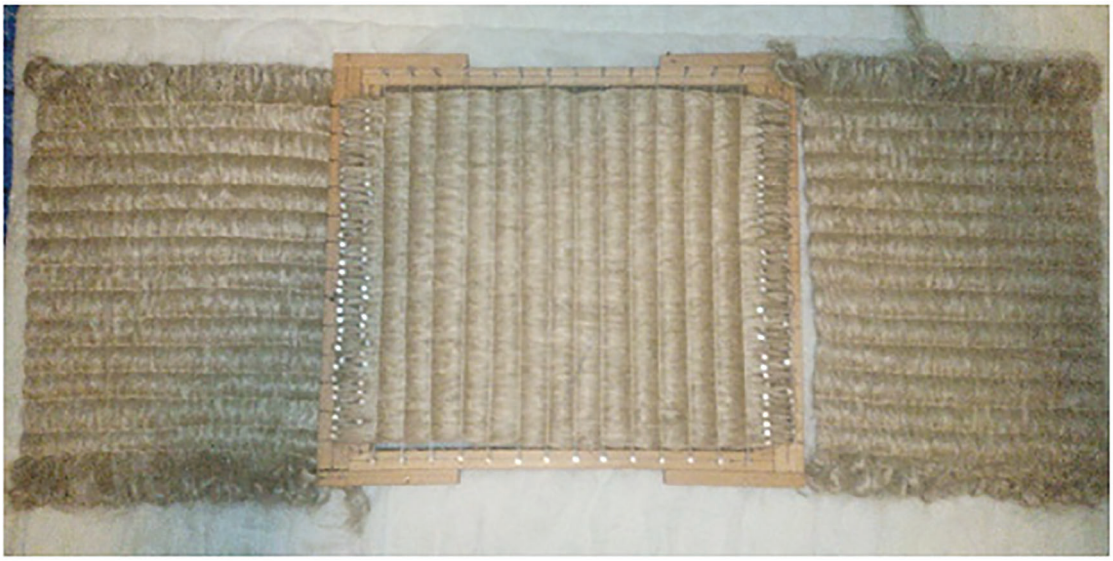

Figure 7: Unidirectional woven mats

3.3.3 Tensile Test

Fig. 8 shows the average tensile curves obtained. There are three zones: a linear zone corresponding to the elastic behavior of the material; a non-linear zone associated with the appearance of initial damage to the matrix and fibers followed by a sudden drop in stress which corresponds to the total rupture of the material. The Young's Modulus MOE was determined using the MATLAB calculator between the values 0.0005 and 0.0025 [38]. Ultimate strength tensile Rm corresponds to the maximum of the curve, yield strength σ_y and yield strain ε_y. The characteristics obtained are mentioned in Tab. 4.

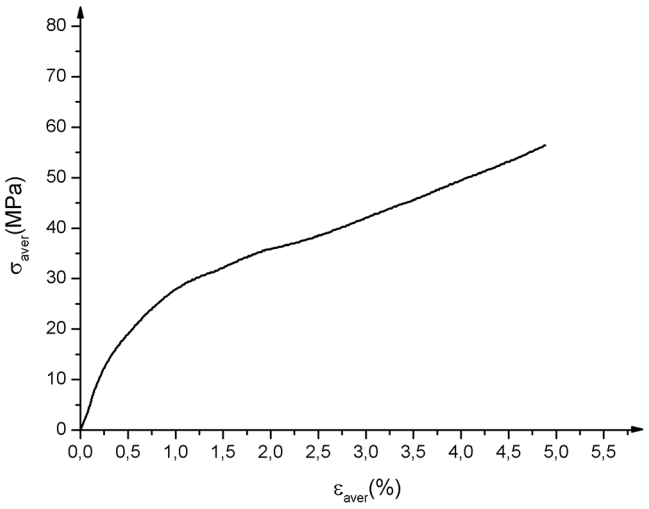

Figure 8: Biocomposites strain-stress tensile test average curves. σ_{aver} and ε_{aver} are respectively average stress and average strain

Table 4: Tensile characteristics of biocomposites

ρ ($kg{\cdot}m^{-3}$)	F_m (kN)	R_m (MPa)	E (GPa)	ε_y (%)	σ_y (MPa)
926	4.6	55	6	0.6	21.50

The different specimens show similar behavior, the average breaking strength is 4.6 kN. There is a slight dispersion of the breaking strength (standard deviation 0.64) This would be mainly due to the existence of defects (air bubbles) caused by the pressing during the curing process (Fig. 9b), and the non-homogeneity and arrangement of fibers during the weaving process. The Young's modulus values are obtained from the linear regression tendency curve of the elastic part.

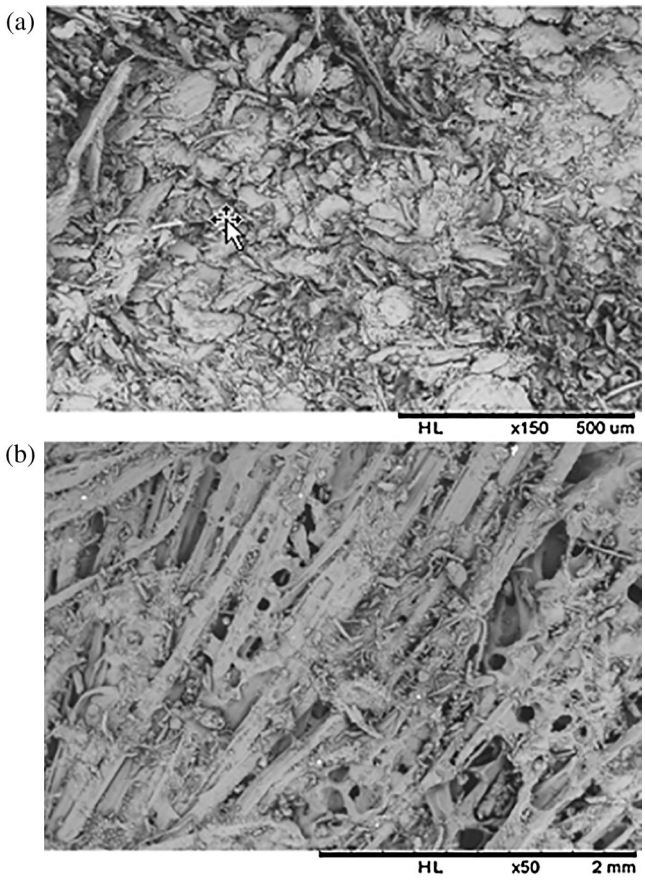

Figure 9: Microstructural analysis of composites by scanning electron microscopy (a) cross section view, Gross magnification: 150 and (b) Longitudinal view, Gross magnification: 50

3.3.4 Scanning Electron Microscopy

Microstructural analysis of section (Fig. 9a) reveals good cohesion between the fiber and the binder, even if sometimes the binder forms an operculum on the fibers. The longitudinal view (Fig. 9b), shows pores, which may be due to the evaporation of the water contained in the resin during thermo-pressing [49].

3.3.5 Bending Test

The 3 points bending behavior of the biocomposite represented in Fig. 10 (average curves) has two main parts and the characteristics are given in Tab. 5. Before microcracking, the behavior is mostly linear elastic, even if diffuse damage already exists within the material. Subsequently, the behavior becomes non-linear due to the progressive increase in the level of diffuse damage (Fig. 10). The microcracks would have propagated rapidly and would have led to a brittle or nearly fragile type fracture. The transfer of loads to the fibers leads to a more or less marked softening or even to a strain-hardening type of behavior. According to tensile and bending characteristics. It could be used as a building exterior structure [50].

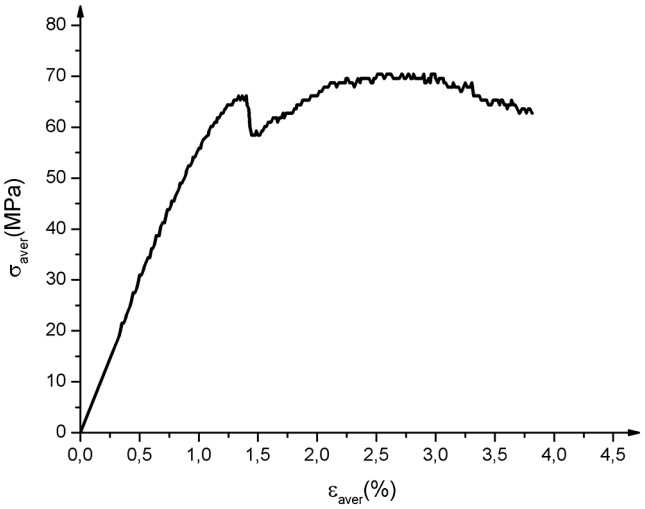

Figure 10: Biocomposites 3-point-bending test average curves. σ_{aver} and ε_{aver} are respectively average stress and average strain

Table 5: Flexural characteristics of biocomposites

$\rho(kg{\cdot}m^{-3})$	*f (mm)*	F_r *(N)*	σ_r *(MPa)*	*E (GPa)*
926	*1.82*	*22*	*68.3*	*9.3*

4 Conclusions

The *Piptadeniastrum Africanum* bark tannin extract is a condensed one consisting of Chalcone; Epicatechin; Apigenin; Fisetinidin; Catechin; Quercetin; Gallocatechin, Epicatechingallate and Epigallocatechin gallate. Used for resin formulation with *Vachellia nilotica* as hardener. The resin developed has interesting mechanicals characteristics. The biohardeners tested have good reactivity with this tannin. The UD mat biocomposite of *urena lobata* fibers elaborated has high-performance with good tensile and bending characteristics. It could be used as a building exterior structure. Thermals properties will be investigated in the future, to know if this material can be used as insulator.

Acknowledgement: The LERMAB of the University of Lorrain. Also, A. Bobbo Director of the Advanced Vocational Training Centres (AVTC) of Douala and Nzogning F. head of Mechanics Department (AVTC Limbe), for equipment and extractions.

Funding Statement: The authors received no specific funding for this study.

Conflicts of Interest: The authors declare that they have no conflicts of interest to report regarding the present study.

References

1. Baley, C. (2005). Fibres naturelles de renfort pour matériaux composites. Techniques de léIngénieur.
2. Bourmaud, A. (2011). *Contribution à l'étude multi-échelles de fibres végétales et de biocomposites (Ph.D. Thesis)*. University of Lorient, France.
3. Drzal, L. T., Mohanty, A., Misra, M. (2001). Bio-composite materials as alternatives to petroleum-based composites for automotive applications. *Magnesium, 40(60),* 1–3.
4. Elouaer, A. (2011). *Contribution à la compréhension et à la modélisation du comportement mécanique de matériaux composites à renfort en fibres végétales (Ph.D. Thesis)*. Université de Reims Champagne-Ardene, France.
5. Kueny, R. (2013). Biocomposites : Composites de hautes technologies en renfort de fibres naturelles et matrice de résines naturelles *(Ph.D. Thesis)*. Université de Lorraine. https://hal.univ-lorraine.fr/tel-01750535.
6. Pizzi, A., Kueny, R., Lecoanet, F., Massetau, B., Carpentier, D. et al. (2009). High resin content natural matrix–natural fiber biocomposites. *Industrial Crops and Products, 30(2),* 235–240. DOI 10.1016/j.indcrop.2009.03.013.
7. Berthelot, J. M. (2010). *Mécanique des matériaux et structures composites*. ISMANS, Institut Supérieur des Matériaux et Mécaniques Avancés, Le Mans, France.
8. Florimond, C., Vilfayeau, J., Vidal-Sallé, E., Boisse, P. (2013). Modélisation numérique du procédé de tissage de renforts fibreux pour matériaux composites.
9. Vilfayeau, J. (2014). *Modélisation numérique du procédé de tissage des renforts fibreux pour matériaux composites (Ph.D. Thesis)*. INSA de Lyon, Français.
10. Anderson, J., Thornback, J. (2012). A guide to understanding the embodied impacts of construction products. *Construction Products Association, 12,* 2013.
11. Morgenstern, O., Stone, K. A., Schofield, R., Akiyoshi, H., Yamashita, Y. et al. (2018). Ozone sensitivity to varying greenhouse gases and ozone-depleting substances in CCMI-1 simulations. *Atmospheric Chemistry and Physics, 18(2),* 1091–1114. DOI 10.5194/acp-18-1091-2018.
12. Konai, N., Pizzi, A., Raidandi, D., Lagel, M. C., L'Hostis, C. et al. (2015). Aningre (Aningeria spp.) tannin extract characterization and performance as an adhesive resin. *Industrial Crops and Products, 77,* 225–231. DOI 10.1016/j.indcrop.2015.08.053.
13. Maison, A., Pasquier, E. (2008). *Le point des connaissances sur le formaldéhyde*. 3e éd. . Paris: Institut National de Recherche et de Sécurité pour la Prévention des Accidents du Travail et des Maladies Professionnelles.
14. Bernard, D. (2002). Resines Naturelles, (K340v2). Techniques Ingénieur. https://www.techniques-ingenieur.fr/base-documentaire/sciences-fondamentales-th8/constantes-chimiques-des-solvants-et-produits-42337210/resines-naturelles-k340/#biblio.
15. Rhazi, N. F. C. (2015). *Mise au point de mélanges collants écologiques à partir des écorces d'Acacia mollissima du Maroc (Ph.D. Thesis)*. Université de Pau et des Pays de l'Adour, Université Hassan II, Casablanca, Maroc. http://www.theses.fr/2015PAUU3049.
16. Saad, H., Charrier, B., Ayed, N., Charrier-El-Bouhtoury, F. (2017). Valorization of Tunisian alfa fibres and sumac tannins for the elaboration of biodegradable insulating panels. *European Physical Journal Applied Physics, 80(2),* 20201. DOI 10.1051/epjap/2017170084.
17. Thébault, M., Pizzi, A., Dumarçay, S., Gerardin, P., Fredon, E. et al. (2014). Polyurethanes from hydrolysable tannins obtained without using isocyanates. *Industrial Crops and Products, 59,* 329–336. DOI 10.1016/j.indcrop.2014.05.036.
18. Roberts, T. (2013). CAFboard compressed-straw panel is back. Using American-made waste straw for wallboard, insulation, and acoustic applications, Stramit USA has brought back CAFboard. *BuildingGreen*. Volume 22; Issue 5, Retrieved March 22, 2020, https://www.buildinggreen.com/product-review/cafboard-compressed-straw-panel-back.
19. El Hajj, N., Dheilly, R. M., Aboura, Z., Benzeggagh, M., Queneudec, M. (2009). Procédé de fabrication des composites 100% végétaux: Effet de la granulométrie des étoupes de lin et de l'ajout des bios liants=

Manufacturing process of 100% vegetable composites: Effect of the flax tow grading and the addition of biological matrix. JNC 16, Toulouse, France.

20. Sauget, A., Zhou, X., Pizzi, A. (2014). Tannin-resorcinol-formaldehyde resin and flax fiber biocomposites. *Journal of Renewable Materials, 2(3),* 173–181. DOI 10.7569/JRM.2013.634128.
21. Ndiwe, B., Pizzi, A., Tibi, B., Danwe, R., Konai, N. et al. (2019). African tree bark exudate extracts as biohardeners of fully biosourced thermoset tannin adhesives for wood panels. *Industrial Crops and Products, 132,* 253–268. DOI 10.1016/j.indcrop.2019.02.023.
22. Ndiwe, B., Pizzi, A., Danwe, R., Tibi, B., Konai, N. et al. (2019). Particleboard bonded with bio-hardeners of tannin adhesives. *European Journal of Wood and Wood Products, 77(6),* 1221–1223. DOI 10.1007/s00107-019-01460-5.
23. Yahmed, D. B. (2010). *Atlas du Cameroun*. Paris: Editions du Jaguar.
24. Jauneau, A., Bert, F., Rihouey, C., Morvan, C. (1997). Les traitements biologiques du lin. *Biofutur, 1997(167),* 34–37. DOI 10.1016/S0294-3506(99)80304-4.
25. Meijer, W., Vertregt, N., Rutgers, B., Van de Waart, M., (1995). The pectin content as a measure of the retting and rettability of flax. *Industrial Crops and Products, 4(4),* 273–284. DOI 10.1016/0926-6690(95)00041-0.
26. Ndiwe, B., Tibi, B., Danwe, R., Konai, N., Pizzi, A. et al. (2020). Reactivity, characterization and mechanical performance of particleboards bonded with tannin resins and bio hardeners from African trees. *International Wood Products Journal, 11(2),* 1–14. DOI 10.1080/20426445.2020.1731070.
27. Navarrete, P., Pizzi, A., Pasch, H., Rode, K., Delmotte, L. (2010). MALDI-TOF and 13C NMR characterization of maritime pine industrial tannin extract. *Industrial Crops and Products, 32(2),* 105–110. DOI 10.1016/j.indcrop.2010.03.010.
28. Xi, X., Pizzi, A., Gerardin, C., Lei, H., Chen, X. et al. (2019). Preparation and evaluation of glucose based non-isocyanate polyurethane self-blowing rigid foams. *Polymers, 11(11),* 1802. DOI 10.3390/polym11111802.
29. Sauget, A., Zhou, X., Pizzi, A. (2014). MALDI-ToF analysis of tannin-resorcinol resins by alternative aldehydes. *Journal of Renewable Materials, 2(3),* 186–200. DOI 10.7569/JRM.2013.634138.
30. Li, X., Pizzi, A., Zhou, X., Fierro, V., Celzard, A. (2015). Formaldehyde-free prorobitenidin/profi setinidin tannin/furanic foams based on alternative aldehydes: glyoxal and glutaraldehyde. *Journal of Renewable Materials, 3(2),* 142–150. DOI 10.7569/JRM.2014.634117.
31. Laigle, Y., Kamoun, C., Pizzi, A. (2009). Particleboard I.B. forcast by TMA bending in UF adhesives curing. *Holz als Roh- und Werkstoff, 56,* 154. DOI 10.1007/s001070050288.
32. Santiago-Medina, F. J., Pizzi, A., Abdalla, S. (2017). Hydroxymethylfurfural hardening of pine tannin wood adhesives. *Journal of Renewable Materials, 5(5)*, 435–447. DOI 10.7569/JRM.2017.634166.
33. Pizzi, A. (1997). On the correlation of some theoretical and experimental parameters in polycondensation cross-linked networks. *Journal of Applied Polymer Science, 63(5),* 603–617.
34. Pizzi, A., Probst, F., Deglise, X. (1997). Molecular mechanics modelling of interfacial energy and flexibility on cellulose. *Journal of Adhesion Science and Technology, 11(4),* 573–589. DOI 10.1163/156856197X00093.
35. Simon, C., Pizzi, A. (2003). Tannins/melamine-urea-formaldehyde (MUF) resins substitution of chrome in leather and its characterization by thermomechanical analysis. *Journal of Applied Polymer Science, 88(8),* 1889–1903. DOI 10.1002/app.12042.
36. NF G07-307 (1987). Textiles. Fiber tests. Determination of the breaking strength of wool fiber bunches. https://www.boutique.afnor.org/norme/nf-g07-307/textiles-essais-des-fibres-determination-de-la-tenacite-de-rupture-des-faisceauxde-fibres-de-laine/article/773944/fa001818.
37. Chanvillard, G. (1999). Caractérisation des performances d'un béton renforcé de fibres à partir d'un essai de flexion. Partie 1: De la subjectivité des indices de ténacité. *Materials and Structures, 32(6),* 418–426. DOI 10.1007/BF02482713.
38. ISO 527-4 (1997). Plastiques–Détermination des propriétés en traction–Partie 4: Conditions d'essai pour les composites plastiques renforcés de fibres isotropes et orthotropes. https://www.iso.org/obp/ui/#iso:std:iso:527:-4:ed-1:v1:fr.

39. NF EN ISO 178 (2019). Textiles. Fiber tests. Determination of the breaking strength of wool fiber bunches. https://www.boutique.afnor.org/norme/nf-en-iso-178/plastiques-determination-des-proprietes-en-flexion/article/904840/fa187233.
40. Saad, H., Charrier-El Bouhtoury, F., Pizzi, A., Rode, K., Charrier, B. et al. (2012). Characterization of pomegranate peels tannin extractives. *Industrial Crops and Products, 40,* 239–246. DOI 10.1016/j.indcrop.2012.02.038.
41. Drovou, S., Pizzi, A., Lacoste, C., Zhang, J., Abdulla, S. et al. (2015). Flavonoid tannins linked to long carbohydrate chains – MALDI-TOF analysis of the tannin extract of the African locust bean shells. *Industrial Crops and Products, 67,* 25–32. DOI 10.1016/j.indcrop.2015.01.004.
42. Tondi, G., Petutschnigg, A. (2015). Middle infrared (ATR FT-MIR) characterization of industrial tannin extracts. *Industrial Crops and Products, 65,* 422–428. DOI 10.1016/j.indcrop.2014.11.005.
43. Hemingway, R. W. (1998). *Practical Polyphenolics: From Structure to Molecular Recognition and Physiological Action By Edwin Haslam (University of Sheffield)*. New York, NY: Cambridge University Press. American Chemical Society.
44. Nkatha, L. (2012). Determination of quality and utilization of Aramine fibers from the plant urena lobata as a textile fiber in Kenya. *Engineering MST-Department of Textiles, Family and Consumer Sciences*. http://ir-library.ku.ac.ke/handle/123456789/3791.
45. Blackburn, R. (2005). *Biodegradable and Sustainable Fibers*. Woodhead Publishing; 1st Edition, Elsevier.
46. Kaswell, E. R. (1963). Wellington sears handbook of industrial textiles. *Wellington Sears Co. New York. N.Y.* 1st Edition. ISBN-13:978-1114317987.
47. Mahato, K., Goswami, S., Ambarkar, A. (2014). Morphology and mechanical properties of sisal fibre/vinyl ester composites. *Fibers and Polymers, 15(6),* 1310–1320. DOI 10.1007/s12221-014-1310-9.
48. Wallenberger, F. T., Weston, N. (2003). *Natural Fibers, Plastics and Composites*. Springer Science & Business Media. DOI 10.1007/978-1-4419-9050-1.
49. Sauget, A. (2014). *Développement de matériaux composites fibreux hautes perfomances à matrice bio-sourcée (Ph.D. Thesis)*. Université de Lorraine, France.
50. Berreur, L., Maillard, D. B., Nösperger, S. (2002). *L'industrie française des matériaux composites*. NODAL CONSULTANTS/DiGTTIP/SIM.